In-situ and post annealing effect on the microstructure and the optical properties of black Cu-Co-Mn oxide spinel coating for Parabolic Trough Collector (PTC) applications

In-situ and post annealing effect on the microstructure and the optical properties of black Cu-Co-Mn oxide spinel coating for Parabolic Trough Collector (PTC) applications

Samaneh Daviran, Anna Krammer and Andreas Schüler

Solar Energy and Building Physics Laboratory (LESO-PB)
Ecole Polytechnique Fédérale de Lausanne, EPFL Station 18, CH-1015 Lausanne, Switzerland

Email address: andreas.schueler@epfl.ch

Abstract. The present paper deals with the deposition of Cu-Co-Mn oxides thin film by magnetron sputtering to produce a black selective coating for solar Parabolic Trough Collector (PTC) systems. The effect of temperature was studied between the nominal temperature range of 300-600°C, using both in-situ heating and post annealing. The optical behavior was investigated by advanced spectrophotometry devices in visible, near and infrared spectral ranges. Scanning Electron Microscopy (SEM) was used to show the microstructure, and X-ray Diffraction (XRD) to identify the phases and to compare the samples'pattern prepared at different temperatures.

1. Introduction

One of the most popular utilizations of solar energy is to convert it into heat. This is because solar energy will not disturb the ecological balance, and the earth receives abundant solar radiation [1]. There are 20 active Parabolic Trough Collector (PTC) power plants worldwide: eleven in Spain, five in USA, two in Iran, one in Italy and one in Morocco [2]. Although parabolic trough collector systems have been mainly utilized for power generation, different other kinds of applications have been reported for such systems like industrial heat processes [3, 4], building heating/cooling [5-11], and water pasteurization [12]. For countries with high irradiation levels, their use for solar cooling can be an attractive investment which is environmental friendly [10].

The building sector is a major energy consumer (32% of global energy use in the world) and it is responsible for more than 30% of total end-use energy related CO_2 emissions (IEA, 2012) [6]. Solar energy utilization is the most widespread renewable method for covering a part of the thermal or electrical needs of the buildings [10]. These two needs can be partially covered by micro combined heat and power (micro-CHP) systems. A micro-CHP prototype has been built in La Rochelle (France) for the purpose of building space heating [6]. A solar assisted absorption heat pump system was installed and studied at Tianjin University in which the primary heat source was supplied from parabolic trough collectors [5]. In reference [8] a proposal for implementation of a PTC system as solar cooling in the building sector was presented. It was found that the solar cooling system can cope with the cooling loads of the buildings under realistic conditions.

On a European level there is intense research activity to broaden the applications of solar thermal systems (hot water, space heating support) and to foster implementation in the EU-Member States. PTC systems are expected to play a key role in this effort [8]. In Switzerland there were also some projects [3] to develop the concentrating solar systems.

In order to reach a high efficiency, the absorber tube of a PTC has to efficiently absorb the incoming radiation but should prevent heat loss by infrared radiation. The coatings should be chemically and

structurally stable within the range of operating temperatures, durable and long lived, comply with any local regulations or restrictions on use of materials for health, easy to apply to the absorber tube and with a good adhesion to the absorber [13]. Kaluza et al. [14] have proposed mixed oxides of Cu-Co-Mn oxides which showed good selectivity. Bayón et al. [15] reported an improvement in the solar absorption of a multilayered coating based on Cu–Mn oxides up to 0.95. Based on the previous studies of our group [16,17], the black Cu-Co-Mn oxide spinel has shown remarkable stability at high temperatures and promising optical properties, which makes it a good candidate for PTC applications. In the present paper, the sputtering temperature and post annealing effect were investigated on properties of the black spinel.

2. Methodology

2.1. Deposition: Magnetron Sputtering

In this study, magnetron sputtering was used as the deposition method. First, aluminum was deposited on silicon wafer as the bottom layer, since it shows high reflectance over the middle infrared region and as a result a low thermal emissivity. Then, the spinel was coated on an aluminum mirror as the absorbing layer. The deposition parameters such as argon and oxygen partial pressure, deposition power, sample and target distance were kept constant for all samples and the temperature was the only variable parameter. The deposition chamber was pumped down to the base pressure of 10^{-7} mbar. A high pure Cu-Co-Mn target with atomic ratio of 1:1:1 was used as the target. The target and the substrate were cleaned using Argon plasma for 5 minutes. Then the deposition was carried out with a 75w pulsed DC power supply for one hour at the pressure of around 10^{-3} mbar. As mentioned above, the effect of both in-situ and post annealing were studied. As for the in-situ heating, the vacuum chamber temperature was set to 300, 400, 500 and 600°C and kept stable for one hour before starting deposition. And in post annealing cases, the deposition was conducted at room temperature and then the samples were post annealed in air at 300-600°C for one hour. The temperature increase in post annealing to the desired temperature was processed with 50°C steps, and then the samples were cooled down at a slow rate of 3-5°C. The deposition parameters are summarized in table 1. The aluminum target was purchased from AJA International Inc. with a diameter of 50.8 mm and a thickness of 6.35 mm. The Cu-Co-Mn target was ordered from Testbourne Ltd, with stoichiometry of 1:1:1, and 50.8 mm in diameter and 3.18 mm in thickness. Both targets present a purity of 99.999%.

Table 1. Deposition parameters

Target	AC /DC	Sample rotation (rpm)	Cleaning power	Cleaning time (min)	Conditioning time (min)	Ar flow (sccm)	O_2 flow (sccm)	Deposition time (min)	Deposition Power (W)	Deposition Temperature (°C)	Deposition pressure (mbar)
Aluminum	Pulsed DC / 250KHz	20	150	3	3	20	-	30	150	room	$5\ 10^{-3}$
Cu-Co-Mn-O	Pulsed DC / 75KHz	20	150	5	5	5	22	60	75	variable	$3\ 10^{-3}$

2.2. Characterization

In this project, the samples were characterized by spectrophotometry. The reflectivity was measured in three steps: visible, near and middle infrared ranges (from 400 to 16000 nm). An integrating sphere and a source emitting isotropic radiation whose intensity distribution is similar to that of a black body (LOT, RT-060-SF), was used for both visible and near infrared spectral ranges. For visible ranges, between 400 and 800 nm, a spectrograph (MultiSpec 125TM 1/8m, Oriel, model 77400) associated to a PDA sensor (Silicon Photodiode Arrays, Intaspec II TM detector head, model 77090) was used. For the near infrared spectral range, a monochromator (Optronic Laboratories, OL 750-MPS) associated with a photosensitive detector Optronic Laboratories, OL 730PbS) was used. Finally, for the middle infrared ranges, between 2500 and 15 400 nm, a Bio-Rad FTS-175C Fourier transform infrared spectrometer equipped with a 3” golden integrating sphere and a high-performance nitrogen-cooled MCT detector was used in order to control the optical properties of the samples. The phase identification was studied

using X-Ray Diffraction (XRD). The microstructure of the film and the elemental analysis were also investigated with Scanning Electron Microscopy (SEM)/Energy Dispersive X-Ray Spectrometer (EDS).

3. Result and Discussion

3.1. Crystalline structure of thin films

Figures 1a and b show XRD spectra of deposited black spinel thin films at different deposition temperatures and different post annealed temperatures. The term of deposition temperature refers to the temperature of the sample in the vacuum chamber in which the substrate was installed. The reference peak locations of Cu-Co-Mn oxide and two prominent peaks of Cu-O are also shown with dashed lines. The diffraction patterns have been analyzed with ICDD database #47-0324 and #48-1548. The spinel can be identified by eight peaks at 18.825°, 30.906°, 38.101°, 44.233°, 54.830°, 58.519°and 64.228°. They can be respectively assigned to the diffraction lines produced by the (111), (220), (311), (222), (400), (422), (511) and (440) planes of Cu-Co-Mn oxide. In all patterns, the sharp peak at 2θ around 54° belongs to the Si sublayer.

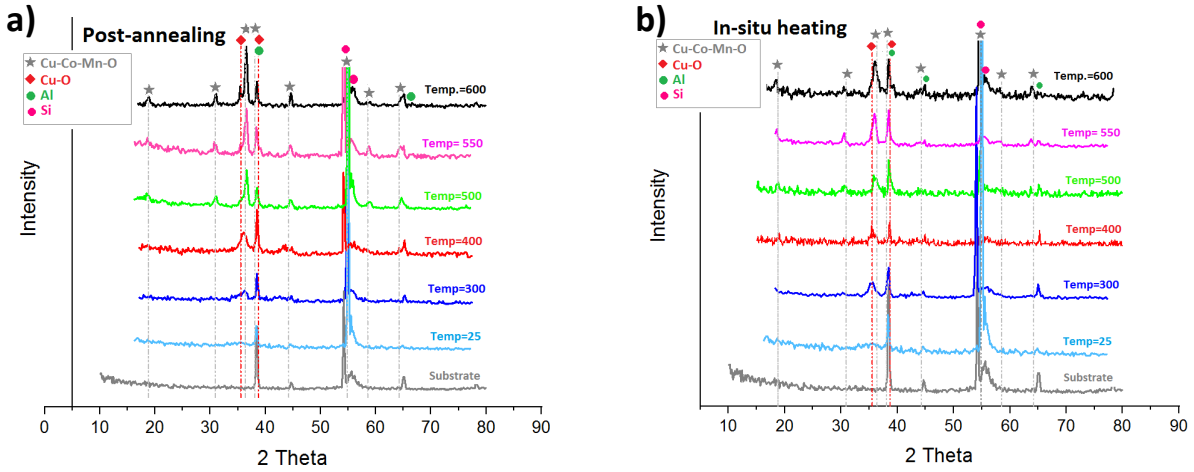

Figure 1. XRD patterns of Cu-Co-Mn oxides thin film deposited on aluminium at different (a) post annealing temperatures, and (b) deposition temperatures which show: Cu-O phase separation at 600°C and 550°C, and spinel phase formation from 400°C and higher

In figure1a the XRD patterns of the spinel thin film deposited at room temperature, 300°C, 400°C, 500°C, 550°C and 600°C are displayed. The film deposited at room temperature shows an amorphous phase with no recognizable spinel peaks, and peaks at 2θ=38.34° and 54.92° are respectively assigned to aluminum and Si sublayers. In the 300°C sample the spinel is in the beginning of crystalline formation and the small peaks at 2θ=36.17° and 44.72° belong to the spinel. By increasing the temperature to 400°C, there was an increase in the mentioned peaks' intensity. In both the 300°C and the 400°C samples two other peaks can be observed at 2θ around 38° and 65°, which can belong to both spinel and the sublayer, aluminium, peaks. The patterns of 500°C, 550°C and 600°C samples show that all eight spinel peaks are formed at higher temperatures. By precise pattern analyzing based on ICDD database #48-1548, the Cu-O phase was identified at 2θ=35.4° for the sample prepared at 600°C. In sample 550°C the Cu-O phase was in the beginning of growing, however it was not observed in sample 500°C.

According to figure 1b, samples that were heated during deposition generally follow a similar behavior in comparison to the post annealed samples. Similar to figure 1a, the Cu-O phase in preferential orientation of (11-1) and (111) at 2θ=35.47° and 38.98° was observed in the pattern of a sample deposited at 600°C, and for the 550°C it is in the beginning of phase separation. Thus, in both cases of post annealing and in-situ heating, the spinel was decomposed at 600°C. In the following the morphology of this case is analyzed using SEM images.

3.2. Microstructure analysis

The desirable properties of absorber coatings are highly dependent on the microstructure of the thin film. To confirm the phase separation of the spinel thin film at 600°C, the microstructure of the sample top surface was detected by SEM. Figure 2 shows the morphology of the sample deposited at 600°C at different scales. In figure 2a, non-uniform sections can be found which have been formed due to the aluminium diffusion. In fact, at high temperatures, aluminium grains grow to the top surface, which makes the surface hazed and results in an adverse effect on the reflectance. This fact is confirmed in the next section. The cross section microstructure of the thin film shown in figure 2d shows that the thickness of the coating is approximately 200 nm. The thin film shows that the surface is relatively porous, and this is one of the reasons that the film has high absorption.

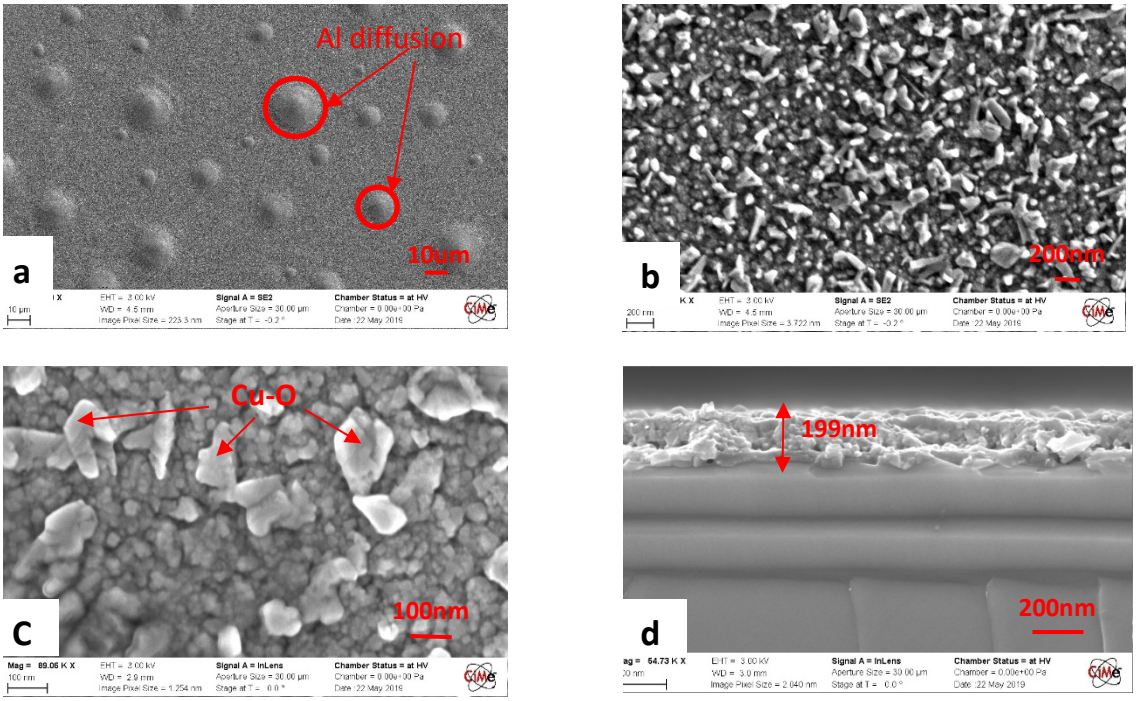

Figure 2. The top and side view morphology of the spinel thin film deposited at 600°C which shows: (a) Al diffusion, (b) larger magnitude of non-diffused background, (c) Cu-O particles in average 200 nm size, (d) cross section view with approximate 200 nm of thickness

In order to better understand the elemental dispersion, the thin film top surface was detected by Energy Dispersive X-Ray Spectrometer (EDS) and the maps were analyzed using AzTech EDS software. As shown in figure 3, the different colors represent different elements of Cu, Co, Mn, Al, and O. The EDS maps show that the distribution of the Co, Mn and O is homogenous. However, a non-uniform distribution of Cu and Al can be observed. The non-uniform distribution of the Al can be explained by its diffusion to the top surface, as it was also shown in SEM images. By comparing figures 3a and 3e, the non-uniformity of the Cu element is compatible to figure 3a, which indicates that the white particles stand for the Cu-O phase.

3.3. Spectrophotometry

The primary objective of this study was to optimize the optical selectivity of the black coating. The deposition power, oxygen partial pressure and the temperature are some important parameters on optical properties of thin film. Based on our previous study, the deposition power and the oxygen flow were kept constant at 75W and 22 sccm, respectively, and only the temperature effect was investigated between the ranges 300-600°C. Figure 4 shows the reflectance measurements for in-situ heated (figure 4a) and post-annealed (figure 4b) samples.

It can be seen that the $\lambda_{Cut-Off}$ is not exactly the same for samples, but all are around 2500nm. This can be explained with close films thickness, because based on Beer Lambert law, the cut-off wavelength is proportional to film thickness and complex part of the refractive index (k). In figure 4a, the trends of all samples at large wavelength, except for 600°C, are quite the same. The reason is that when $\lambda \gg k.d$, the absorption is negligible and the film behaves as a transparent film. So, the measured values show the sublayer reflectance, which here is the opaque aluminium. In both figures, the 600°C sample displays different behavior at middle infrared ranges. As mentioned, at higher wavelength the measurements show the aluminium reflectance. Moreover, based on the SEM results, the aluminium was diffused at 600°C. The aluminium diffusion, increase in surface roughness, phase segregation, and larger grains at 600°C are the parameters which justify the lower reflectance of this sample.

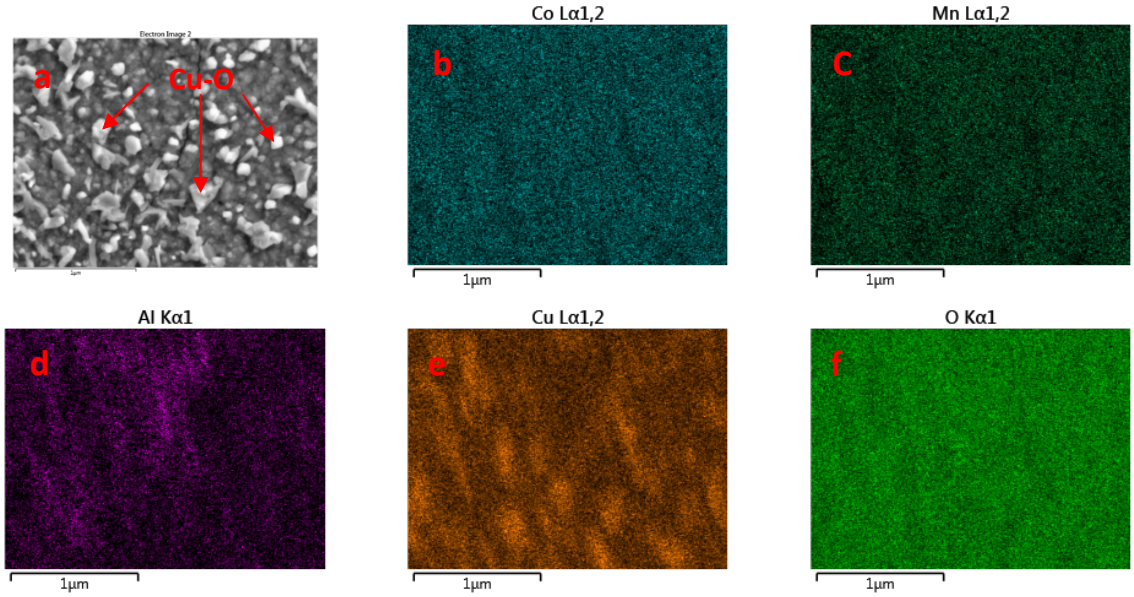

Figure 3. EDS maps images of Cu-Co-Mn oxide thin film deposited on Al mirror, (a) SEM image, (b,c,f) uniform dispersion of Co, Mn, and O, (d) non-uniform Al dispersion which confirms Al diffusion, (e) non-uniform distribution of Cu, which the structure is compatible to figure 3(a) and confirms the Cu-O phase separation

On the other hand, when $\lambda \ll k.d$, the absorption is non negligible. By comparing the reflectance in the visible range, samples at 500°C and 600°C in both in-situ and post annealing show lower reflection values and as a result higher absorption. This can be explained with the morphology of the spinel. The high temperature promotes grain growth and as a result it may make the film more porous. The pores provide light trapping and consequently re-refraction of the wavelength in the pores increase the film absorption.

In near infrared range, the λ_{min} value is not the same for the all curves. The λ_{min} is proportional to film thickness, film refractive index and substrate refractive index. The thickness and refractive index for the substrate is the same for all samples. However, the refractive index of the film can be different because of the oxidation effect. As for the film thickness, although a constant deposition power was used for all samples, which is expected to make films with equal thickness, the thickness can be different because of grain growth at different temperature. Thus, the shift in location of λ_{min} can be explained with both oxidation effect and with the little difference in film thicknesses.

4. Conclusion

In this paper, Cu-Co-Mn oxide used as the black coating for PTC applications. The effect of temperature was studied between the nominal range of 300-600°C, using both in-situ heating and post annealing. The following conclusions can be drawn:

- Based on XRD patterns, the spinel was decomposed at 600°C in both in-situ heating and post-annealing cases. The EDS maps also confirmed the presence of Cu-O phase. The sample deposited at 550°C, was in the beginning of phase separation. In the pattern of sample deposited at 500°C spinel peaks were found, however Cu-O phase was not observed.
- The SEM image showed the aluminum diffusion at 600°C, which can highly affect the film selectivity. This fact was confirmed by spectrophotometry results.

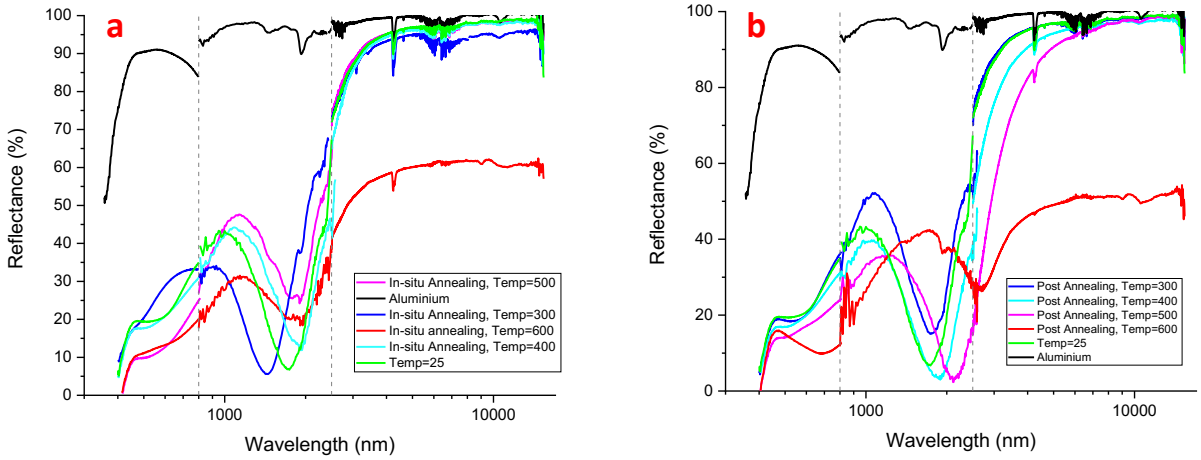

Figure 4. Reflectance spectra at visible, near infrared and middle infrared ranges and comparison of samples at different temperatures for both (a) In-situ heating and (b) Post-annealing cases

- A comparison between reflectance of in-situ heated and the post annealed samples indicates that the in-situ heated sample at 500°C is more promising than the others. This result is obtained by focusing especially on visible and middle infrared ranges. The XRD results also propose 500°C as the appropriate temperature.
- To sum up, two suggestions can be proposed for the future studies. First, existence of excess Cu can facilitate the Cu-O formation. Hence, stoichiometry optimization is required to prevent phase separation. Also, aluminium is not stable at high temperatures and even if the spinel is enough thermally stable, the substrate diffusion disturbs the film selectivity. Thus, developing a thermally stable substrate, which at the same time keeps the reasonable optical properties (high IR-reflectance), is proposed as a future research.

References

[1] Zhang K, Hao L, Du M, Mi J, Wang J N and Meng J P 2017 *Renewable and Sustainable Energy Reviews* **67** 1282–99.
[2] Pavlović T M, Ivana S, Dragana D R, Milosavljević and Lana S P 2012 *Renewable and Sustainable Energy Reviews* **16** 3891-3902.
[3] Larcher M, Rommel M, Bohren A, Frank E and Minder S 2014 *Energy Procedia* **57** 2804-11.
[4] Kizilkan O, Kabul A and Dincer I 2016 *Energy* **100** 167-176.
[5] Wang F, Feng H, Zhao J, Li W, Zhang F and Liu R 2015 *Energy Procedia* **70** 529-36.
[6] BouvierG, P, T and Rochier D 2016 *Solar Energy* **134** 180-92.
[7] Bouvier J L 2016 Étude expérimentale d'une installation de micro-cogénération solaire couplant un concentrateur cylindro-parabolique et un moteur à cycle de Hirn *Doctoral Thesis*.
[8] Drosou V, Kosmopoulos P and Papadopoulos 2016 *Renewable Energy* **97** 697-708.
[9] Balghouthi M, Hadj Ali A B, Trabelsi S, Guizani A 2014 *Energy Conversion and Management* **86** 1134-46.
[10] Tzivanidis C and Bellos E 2016 *Case Studies in Thermal Engineering* **8** 403–13.
[11] Ayadi O, Aprile M and Motta M 2012 *Energy Procedia* **30** 875–83.
[12] Bigoni R, Kötzsch S, Sorlini S and Egli T 2014 *Journal of Cleaner Production* **67** 62–71.
[13] Atkinson C, Sansom C L, Almond H J and Shaw C P *Renewable and Sustainable Energy Reviews* **45** 113–22.
[14] Kaluza L, Orel B, Drazic G and Kohl M 2001 *Solar Energy Materials and Solar Cells* **70** 187–201.
[15] Bayón R, Vicente G S and Morales Á 2010 *Solar Energy Materials and Solar Cells* **94** 998–1004.
[16] Joly M, Antonetti Y, Python M, Gonzalez M, Gascou T, Scartezzini J L and Schüler A 2013 *Solar Energy* **94** 233–39.
[17] Joly M, Bouvar O, Gascou T, Antonetti T, Python M, González M, Loesch P, Hessler-Wyser A and Schüler A 2015 *Solar Energy Materials & Solar Cells* **143** 573–80.